Scanning Tunneling Spectroscopy of Individual Iron Atoms on a Permalloy Surface

M. Dreyer, H. Pandana, and R. D. Gomez

***Abstract*—The topographic and electronic structure of 10–20-nm-thick permalloy films has been investigated under ultrahigh vacuum conditions. The films were characterized using scanning tunneling microscopy/spectroscopy. Permalloy grows as a polycrystalline film. The size of the crystallites is in the range of 5–20 nm for the permalloy films. The spectroscopic data show a distinct minority electron state, which can be assigned to the presence of iron in the permalloy surface. It was found that the state not only decays but also shifts in position when moving the STM tip away from the center position of the iron atoms.**

***Index Terms*—Chemical identification, permalloy, scanning tunneling microscopy, scanning tunneling spectroscopy.**

I. Introduction

IN RECENT years, there has been a growing interest in the development of spintronics devices [1], where the spin of the electrons is exploited for information processing. A crucial character of an optimized device is the efficient injection of spin-polarized electrons from a highly spin polarized material into a material showing a long spin coherence time. In addition to its magnetic structure, the roughness of the interface and the spin-polarized density of electron states are important for this process. Both issues are addressed in this study.

In a recent report [2], photoemission data were compared with theoretical calculations of the element specific and spin-resolved electronic density of states (DOS) of permalloy. It was shown that a charge transfer from the iron to the nickel leads to a slight enhancement of the majority states at the nickel positions and pronounced increase of the minority states at the iron positions. Furthermore, the shape and position of the iron minority state was found to depend on the iron concentration. In this study, we employed a scanning tunneling microscopy/spectroscopy (STM/STS) system to observe this effect on a local scale on the sample surface, although caution must be taken when comparing "bulk" calculation with data from a surface sensitive measurement. In the case of permalloy, however, the band structure calculations given in [2] also showed a gap of about 1 eV at the Γ-point of the Brillion zone, which is a premise for the observation of possible surface states in STS. Therefore, possible changes in the expression of the charge transfer from nickel to iron should be observable as well. Due to its magnitude, the empty iron bulk state should also show some reminiscence at the sample surface. The probability of not having at least one iron atom within the electronic screening length of the order of $\lambda = 5 - 10$ Å [3], [4] is $5.1 \cdot 10^{-4} - 1.8 \cdot 10^{-18}$ for $Ni_{80}Fe_{20}$. In other words, it is almost certain to find at least one iron atom within a radius of λ of the tip position. Still, the short screening length should allow a clear distinction between surface and subsurface iron.

Manuscript received December 18, 2002. This work was supported in part by the NSF CAREER award under Grant ECS 9984797.

The authors are with the Department of Electrical and Computer Engineering, University of Maryland, College Park, MD 20740 USA (e-mail: dreyer@lps.umd.edu; hpandana@glue.umd.edu; rdgomez@ece.umd.edu).

Digital Object Identifier 10.1109/TMAG.2003.816182

II. Experimental Techniques

The experiments were performed inside a two chamber UHV system at a base pressure of $p_0 < 10^{-10}$ mbar. The chambers are separated by a gate valve. One chamber equipped with two electron beam evaporators and a sample heater is dedicated to sample preparation; the other is used exclusively for sample analysis and storage. The surface-sensitive analytical tools we used were a low-energy electron diffraction (LEED)/Auger electron spectroscopy (AES) system as well as a combined STM/atomic force microscope (AFM). The latter instrument could also be operated in magnetic force microscopy (MFM) mode. For the STM/STS measurements etched tungsten wires were used. The tips were cleaned prior to use by electron beam heating.

The silicon substrates were cleaned by flash heating to 1200 °C for 30 s and subsequent cooling to room temperature to obtain a clean Si (001) surface [5]. The permalloy $(Ni_{80}Fe_{20})$ films were deposited by electron beam evaporation at rates of 0.1–0.3 nm/s from a $Ni_{81}Fe_{19}$ precursor. The ultrathin films with a thickness of 10–20 nm were then characterized *in situ* using STM/STS as well as LEED and AES. The STS data were collected by measuring the first derivative of the current with respect to the bias voltage $(dI/dU_{\rm bias})(U_{\rm bias})$ using a lock-in amplifier. Typical parameters of the modulation frequency and amplitude were $f_{\rm mod} = 1280$ kHz and $A_{\rm mod} = 125$ mV, respectively. The current $I(U_{\rm bias})$ was simultaneously recorded. All spectroscopic data shown are normalized by the conductance, i.e., $(dI/dU_{\rm bias})/(I/U_{\rm bias})$. The resulting quantity is directly proportional to the local density of electron states [6]. The bias voltage was applied at the sample. Negative bias voltage induces tunneling of electrons from the sample to the tip and vice versa. Consequently, the normalized STS data taken at negative (positive) bias voltages corresponds to occupied (empty) electron states of the sample. As is the case in most STM analysis, the electronic structure of clean Tungsten is assumed to be similar to a spherically symmetric ground (hydrogenic-like) state.

0018-9464/03$17.00 © 2003 IEEE

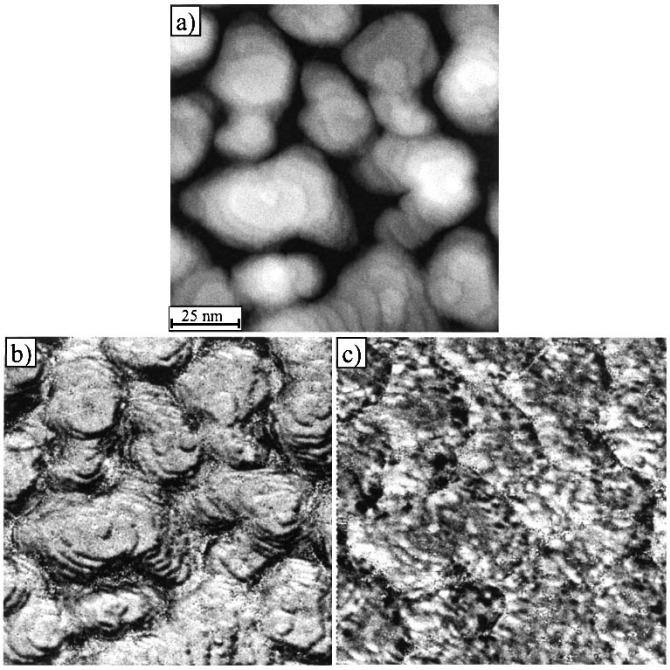

Fig. 1. (a) Topography and simultaneously obtained spatially resolved differential resistance measurements at bias voltages of (b) -0.6 V and (c) $+0.7$ V of 12-nm-thick polycrystalline permalloy film.

III. Results and Discussion

A typical example of the topography as measured by STM is displayed in Fig. 1(a). The samples show polycrystalline structure with a diameter of the individual crystallites ranging from 5–20 nm. The crystallites are randomly oriented, which was also confirmed by the absence of patterns in the LEED measurements. The observed monatomic step heights are consistent with step heights expected for fcc nickel crystallites of 1.76, 2.49, and 2.03 Å for a (100), (110), and (111) oriented surface, respectively. The (111) surface was found readily throughout the surface, while the (110) surface was rarely observed. The measurements of the local density of states (LDOS) at a fixed bias voltage were taken simultaneously with the topography by recording the output voltage of the lock-in amplifier. Two examples measured at bias voltages of -0.6 and $+0.7$ V of the same region of the sample as Fig. 1(a) are shown in Fig. 1(b) and (1c), respectively. The striking dissimilarity of the two images demonstrates the effects of the local density of states. While the monatomic steps are the most pronounced feature visible in the occupied LDOS ($U_{\mathrm{bias}} = -0.6$ V), the empty states ($U_{\mathrm{bias}} = +0.7$ V) show numerous white spots that are also present on top of flat terraces. We assume that the spots are due to the enhancement in the empty local density of states arising from the iron atoms on the sample surface. Contamination from other sources can be ruled out, as AES measurements performed subsequently to the STM measurements showed only the signature of iron and nickel. Furthermore, atomically resolved STM images taken simultaneously show no sign of surface contamination at the location of the enhanced LDOS.

The observed bright regions were further investigated by performing STS on top of larger monatomic flat terraces. Using the unoccupied iron state as a marker, the spectroscopy curves

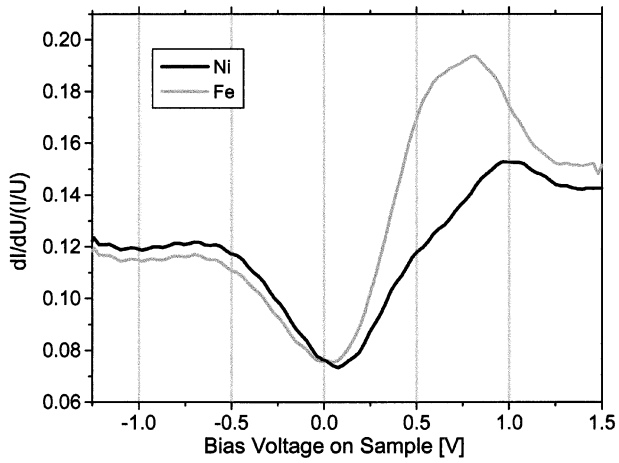

Fig. 2. Plot of averaged spectroscopy curves taken at nickel-rich and iron-rich sites.

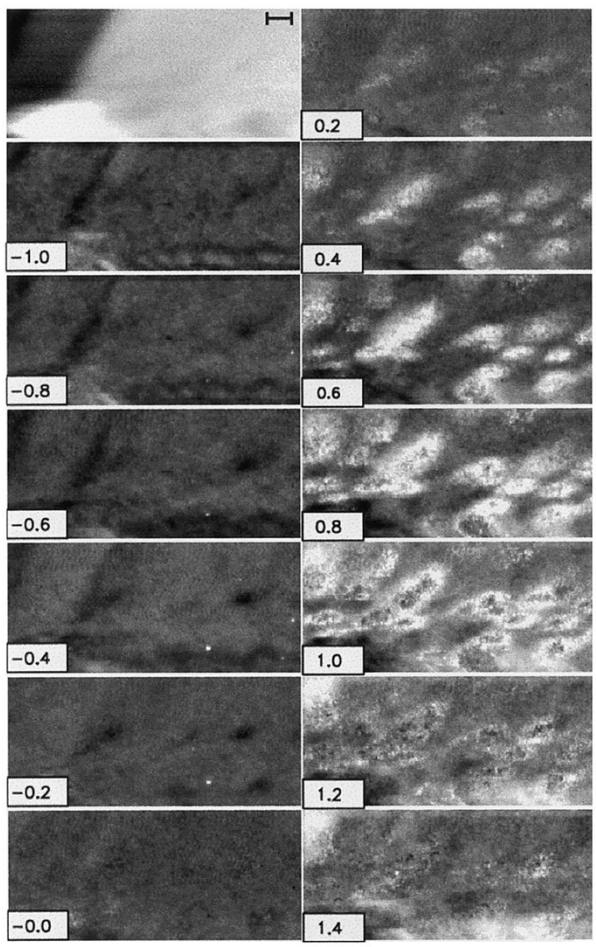

Fig. 3. Topography (top left) and spatially resolved local density of states at -1 to 1.2 V in 0.2-V intervals. Length of the marker in the topographic image is 1 nm.

can easily be divided into two categories as shown in Fig. 2. The plots represent averaged spectra taken at the iron-rich or nickel-rich locations on the sample surface. The tip was stabilized at a bias voltage of $U_{\mathrm{bias}} = -1.3$ V and a tunneling current of $I = 500$ pA above the sample surface before each measurement. The curves show only a small difference in the occupied

states with a shallow peak around $U_{\rm bias} = -0.6$ V and a decreased density of states around the Fermi level. The unoccupied side of the LDOS show a broad peak for iron-rich regions at $U_{\rm bias} = 0.5 - 1.0$ V and a smaller peak at about $U_{\rm bias} = 1$ V in the nickel-rich areas. The "nickel-rich" curve agrees well with what is to be expected from the calculated LDOS shown in [2]. The shallow peak found at a bias voltage of 1 V corresponds to the empty iron state found in the bulk for $Ni_{80}Fe_{20}$ permalloy. On the other hand, the peak in the "iron" curve occurs at approximately 0.7 V, which is at a lower energy than predicted by theory [2]. We postulate that iron in a nickel matrix exhibits a surface state, which is responsible for this low energy peak. Interestingly, it can be used for locating iron.

In order to examine the lateral dependence of the local density of states—especially of the newly found iron surface state—high spatial resolution spectroscopic data are shown in Fig. 3, along with topography. The topography of the region (top left) shows a monatomic step in the upper left corner of a height of 1.8 Å. The step height is consistent with an (100) orientation of the surface. The flat surface shows an average corrugation of 0.3 Å. The images of the occupied LDOS in a range of the bias voltage of $U_{\rm bias} = -1.0 \ldots 0.0$ V are shown in the left column. The monatomic step is visible in as a dark line. On the terrace itself some dark spots indicate a local decrease of the electron density. The empty state images are found on the right side panels. They show the emergence of bright regions, which increase in intensity up to a bias voltage of about $U_{\rm bias} = 0.6$ V. At bias voltages above 0.6 V, the bright spots split up to form ring like structures. The ring structures are due to a shift of the energetic position of the iron surface state from 0.5 to about 0.8 eV when moving the STM tip approximately 0.5 nm away from the iron location with a slow decay in magnitude.

IV. Conclusion

This work demonstrates, for the first time, that it is possible to locate iron atoms in a $Ni_{80}Fe_{20}$ permalloy surface by means of STS and opens the possibility for observing individual atoms. On the surface of the sample, the displacement of one of the electrons of iron toward the nickel atoms leads to the formation of a pronounced surface state. This state is easily observable in STS, and the energy dispersion of that surface state was found. DOS and band structure calculations would be helpful to fully understand the observed electronic structure.

References

[1] G. A. Prinz, *Science*, vol. 282, p. 1660, 1998.
[2] P. E. Mijnarends, S. Sahrakorpi, M. Lindroos, and A. Bansil, "Angle-resolved photoemission spectra, electronic structure, and spin-dependent scattering in $Ni_{1-x}Fe_x$ permalloys," *Phys. Ref. B*, vol. 65, p. 075 106, 2002.
[3] G. Landry, Y. Dong, J. Du, X. Xiang, and Q. Xiao, "Interfacial capacitance effects in magnetic tunneling junctions," *Appl. Phys. Lett.*, vol. 78, pp. 501–503, 2001.
[4] S. Zhang, "Spin-dependent surface screening in ferromagnets and magnetic tunnel junctions," *Phys. Ref. Lett.*, vol. 83, pp. 640–643, 1999.
[5] B. S. Swartzenhuber, Y.-W. Mo, M. W. Webb, and M. G. Lagally, "Scanning tunneling microscopy studies of structural disorder and steps on Si surfaces," *J. Vac. Sci. Technol. A*, vol. 7, pp. 2901–2905, 1989.
[6] V. A. Ukraintsev, "Data evaluation technique for electron-tunneling spectroscopy," *Phys. Ref. B*, vol. 53, p. 11 176, 1996.